

**Characterization of
limonene ozonolysis
SOA**

S. Kundu et al.

**High molecular weight SOA formation
during limonene ozonolysis: insights
from ultrahigh-resolution FT-ICR mass
spectrometry characterization**

S. Kundu^{1,2}, R. Fisseha³, A. L. Putman³, T. A. Rahn³, and L. R. Mazzoleni^{1,2}

¹Department of Chemistry, Michigan Technological University, Houghton, MI 49931, USA

²Atmospheric Science Program, Michigan Technological University, Houghton, MI 49931, USA

³Earth and Environmental Sciences Division, Los Alamos National Laboratory, Los Alamos, NM 87545, USA

Received: 5 January 2012 – Accepted: 7 January 2012 – Published: 24 January 2012

Correspondence to: L. R. Mazzoleni (lrmazzol@mtu.edu)

Published by Copernicus Publications on behalf of the European Geosciences Union.

Title Page

Abstract

Introduction

Conclusions

References

Tables

Figures

◀

▶

◀

▶

Back

Close

Full Screen / Esc

Printer-friendly Version

Interactive Discussion



Abstract

The detailed molecular composition of secondary organic aerosols (SOA) from limonene ozonolysis was studied using ultrahigh-resolution Fourier transform ion cyclotron resonance (FT-ICR) mass spectrometry. High molecular weight (MW) compounds ($m/z > 300$) were found to constitute a significant number fraction of the identified SOA components. Double bond equivalents (DBE = the number of rings plus the number of double bonds) increased with MW. The O:C ratios and relative abundances of compounds decreased with increasing MW. The mass spectra of limonene contain 4 distinct clusters of negative ions: Group I ($140 < m/z < 300$), Group II ($300 < m/z < 500$), Group III ($500 < m/z < 700$) and Group IV ($700 < m/z < 850$). A number of CH_2 and O homologous series of low MW SOA (Group 1) with carbon number 7–15 and oxygen number 3–9 were observed. Their occurrence can be explained with isomerization and elimination reactions of Criegee radicals, reactions between alkyl peroxy radicals, and scission of alkoxy radicals resulting from the Criegee radicals. Additionally, fragmentation analysis and observations of formaldehyde homologous series provide evidence for aerosol growth by the reactive uptake of generated gas-phase carbonyls in limonene ozonolysis. The decreasing O:C ratios between group of compounds indicated the importance of condensation (aldol and esterification) reaction pathways for high MW compound formation. However, the prominent DBE changes of 2 between the groups of compounds and selected fragmentation (MS/MS) analysis of Group II and Group III ions indicated a predominance of non-condensation (hydroperoxide, Criegee and hemi-acetal) reaction pathways. A reaction matrix created with the combination of low MW SOA, hydroperoxides, and Criegee radicals indicated higher frequencies for the hemi-acetal and condensation reaction pathways. Overall, the combined approach confirms the importance of non-condensation reaction pathways over condensation reaction pathways. Among the non-condensation reaction pathways, hemi-acetal reactions appear to be most dominant followed by hydroperoxide and Criegee reactions.

Characterization of limonene ozonolysis SOA

S. Kundu et al.

Title Page

Abstract

Introduction

Conclusions

References

Tables

Figures

◀

▶

◀

▶

Back

Close

Full Screen / Esc

Printer-friendly Version

Interactive Discussion



1 Introduction

Organic aerosols, constituting up to 90 % of the aerosol mass fraction, are known to have adverse impacts on visibility, climate, public health and biogeochemistry (Kanaki-dou et al., 2005; Salma et al., 2008). Total global biogenic secondary organic aerosols (SOA) are estimated to be 12–70 Tg yr⁻¹, greatly exceeding the 2–12 Tg yr⁻¹ of anthropogenic SOA (Hallquist et al., 2009). Since the discovery of aerosol formation from biogenic volatile organic compounds (Went, 1960), significant research has been conducted on the composition of SOA and their formation processes. An improved understanding of the molecular composition and formation processes of SOA is required for a quantitative assessment of its production, properties and environmental effects (Fuzzi et al., 2006). The major biogenic volatile organic compounds consist of isoprene followed by monoterpenes and sesquiterpenes (Liao et al., 2007). Limonene accounts for ~20 % of the total monoterpene emissions into the atmosphere by vegetation (Stroud et al., 2005). Despite its low concentration, limonene has high potential to form SOA because of the presence of an endocyclic and an exocyclic bond. The aerosol yields of limonene ozonolysis are several times higher than those of other monoterpene ozonolysis (Iinuma et al., 2004; Leungsakul et al., 2005; Heaton et al., 2007). Thus due to the significant emissions and higher reactivity of limonene, limonene oxidation may contribute substantially to aerosol organics. Despite their significance, little is known about the molecular composition of biogenic SOA and their formation processes.

Current studies indicate that high MW SOA components are accretion products of low MW components. Therefore, the low MW compounds are often considered to be building units of high MW compounds. To improve our understanding of this process, comprehensive characterization of the low MW SOA components is needed. Several compounds in the mass range of 168 < *m/z* < 202 were detected by Leungsakul et al. (2005) and Geddes et al. (2010) in limonene ozonolysis SOA using a gas chromatography/mass spectrometry (GC-MS) and near-infrared laser desorption/ionization aerosol mass spectrometry (NIR-LDI-AMS). They described the formation of the

Characterization of limonene ozonolysis SOA

S. Kundu et al.

Title Page

Abstract

Introduction

Conclusions

References

Tables

Figures



Back

Close

Full Screen / Esc

Printer-friendly Version

Interactive Discussion



observed compounds with elimination and isomerization reactions of Criegee radicals. In another study using high resolution mass spectrometry, Walser et al. (2008) observed a higher number of low MW components in SOA from limonene ozonolysis. They described the formation of additional compounds with alkyl peroxy and alkoxy radical reactions. Despite the additional pathways, the observed CH₂ and O Homologous series (Walser et al., 2008; Bateman et al., 2009) of low MW components were not fully explained. This suggests a need to characterize the SOA products in more detail and to revisit the reaction schemes for the formation of low MW SOA.

As stated previously, high MW SOA components can be formed by the reactions of low MW neutral molecules with hydroperoxides or Criegee radicals (Ziemann et al., 2005; Docherty et al., 2005). High MW SOA can also be formed by hemi-acetal, and condensation (aldol and esterification) reactions (Iinuma et al., 2004; Gao et al., 2004; Kalberer et al., 2004; Hamilton et al., 2006; Surratt et al., 2006). Heaton et al. (2007) observed the formation of high MW SOA within 3–22 s after ozone and limonene were introduced into a flow reactor. They interpreted the high MW SOA production to result from the hydroperoxide and Criegee reaction channels with a predominance of hydroperoxide reactions. In another study, Bateman et al. (2009) suggested the importance of the Criegee and hemi-acetal reaction pathways for high MW SOA formation in limonene ozonolysis. The hemi-acetal and condensation reaction pathways have also been proposed for the formation of high MW SOA from other monoterpenes (Iinuma et al., 2004; Reinhardt et al., 2007), and isoprene (Surratt et al., 2006). The variety of reaction pathways and conclusions prompt a need for further evaluation of the relative significance of the proposed reaction pathways with respect to the formation of a wide variety of high MW SOA.

A number of approaches to interpret the observed SOA molecular composition and high MW compound formation have been described in the literature. Reinhardt et al. (2007) observed a decrease in the O:C ratios with increasing MW in α -pinene ozonolysis SOA. Similarly, Putman et al. (2011) observed a decrease in the O:C ratios in α -pinene ozonolysis but no decrease in the H:C ratios. Elemental ratios of

Characterization of limonene ozonolysis SOA

S. Kundu et al.

Title Page

Abstract

Introduction

Conclusions

References

Tables

Figures

◀

▶

◀

▶

Back

Close

Full Screen / Esc

Printer-friendly Version

Interactive Discussion



oxygen and hydrogen to carbon (O:C and H:C) decrease with the elimination of water as expected in the condensation reactions (aldol condensation and esterification). The decrease in the O:C with increasing MW is in contrast to the interpretation by Jimenez et al. (2009). Using aerosol mass spectrometry, they report highest O:C ratios for low-volatility OOA (oxygenated organic aerosol), which likely contained a large fraction of oligomeric and other high MW products. Bateman et al. (2009) observed a predominance of double bond equivalents (DBE = the number of rings plus the number of double bonds) to increase by 2 for each groups (monomers, dimers and trimers). DBE increases of 2 are expected for the Criegee, hydroperoxide and hemiacetal reaction pathways, whereas DBE increases of 3 indicate condensation reactions. However, a complex array of building units with different DBE values may result in a complex array of high MW compounds with various DBE values. Heaton et al. (2007) created a reaction matrix of building units to explain the observed high MW compound formation in monoterpene (β -pinene, carene, limonene and sabinene) ozonolysis SOA. This approach resulted in individual high MW compounds formed by different reaction channels. These results suggest a need for a more advanced approach to explain the high MW compound formation.

Here we present the results of ultrahigh-resolution FT-ICR MS analysis with a resolving power of 400 000 to characterize limonene ozonolysis SOA. Reaction pathways and their relative significance for the formation of organic compounds are discussed. Fragmentation analyses with ultrahigh resolution FT-ICR MS were carried out for selected negative ions for structural elucidation and further insights toward an improved understanding of the formation of high MW limonene ozonolysis SOA.

Characterization of limonene ozonolysis SOA

S. Kundu et al.

Title Page

Abstract

Introduction

Conclusions

References

Tables

Figures

◀

▶

◀

▶

Back

Close

Full Screen / Esc

Printer-friendly Version

Interactive Discussion



2 Experimental

2.1 SOA generation and extraction

Aerosol samples were generated by the reaction of ozone and (R)-(+)-limonene (99 %, Sigma-Aldrich) at the Los Alamos National Laboratory in an aerosol chamber. Briefly, the aerosol chamber is 1.5 m³ flexible Teflon bag (5 ml) suspended on a bench top. The chamber was completely covered with a black fabric to simulate dark condition. Before the start of an experiment, the chamber was cleaned by flushing it with purified compressed air (prepared by the Los Alamos National Laboratory gas facility) until the particle number was below 2 particles cm⁻³. Compressed air was purified by passing it through a water trap (Drierite) and hydrocarbon trap (Restek). A condensation particle counter (CPC, TSI 3025A) was used to determine the number of particles. Prior to introduction of reactants, the proper relative humidity was achieved (0 or 4%) and was recorded by a relative humidity sensor (Vaisala Combined Pressure, Humidity and Temperature Transmitter, PTU300). Aerosols were generated under dry conditions to reduce the complexity of SOA formation (Jonsson et al., 2008). Liquid limonene was introduced through a heated port and was allowed to disperse throughout the chamber for 15 min. The target concentration of 500 ppb corresponded to a liquid volume of 4 μ l. Ozone was produced until a maximum concentration of 250 ppb was achieved (Ozone monitor, 2B Technologies, Model 205). Aerosol particles were observed within seconds after ozone was introduced to the chamber. No seed aerosols or hydroxyl radical scavenger were added. The reactants were allowed to react for an hour. A heat mat, maintained at 25–28 °C, was used below the chamber to mix the reactants homogeneously throughout the chamber. The resulting aerosols were collected at a flow rate of 6 slpm for 2.5–5 h on a pre-baked quartz fiber filter. No denuder was used before the aerosol sampler. Chamber blanks were collected following the same methods except limonene and ozone were not added into the chamber. The filters were placed in petri dishes (Pall Corporation) wrapped with aluminum foil and stored frozen until extraction. Samples were kept cool during transport between laboratories.

Characterization of limonene ozonolysis SOA

S. Kundu et al.

Title Page

Abstract

Introduction

Conclusions

References

Tables

Figures

◀

▶

◀

▶

Back

Close

Full Screen / Esc

Printer-friendly Version

Interactive Discussion



SOA and blank samples were extracted with 5 ml of 1:1 mixture of acetonitrile and water. The extraction was carried out in a sonicating bath for 30 min. Extracts were then filtered and stored at -5°C until analysis.

2.2 Ultrahigh-resolution FT-ICR MS analysis

5 Samples were analyzed with a hybrid 7T FT-ICR MS (LTQ FT Ultra, Thermo Scientific) equipped with an electrospray ionization (ESI) source. The instrument was externally calibrated in the negative ion mode with standard solutions of sodium dodecyl sulfate and taurocholic acid and the resulting mass accuracy was better than 2 ppm. Diluted samples were infused at $5\ \mu\text{l}\ \text{min}^{-1}$ into the ESI interface. The ESI probe was placed
10 in position "B", the needle voltage was set between at -3.7 and -4.0 kv and no sheath gas was used. Mass resolving power was set at 400 000 (at mass-to-charge (m/z) 400) for all spectra. The capillary temperature was maintained at 265°C . Mass spectra of m/z 100–1000 were acquired in the negative ion mode. Note that lower intensities of low MW ions ($m/z < 200$) relative to higher ones were observed in the FT-ICR MS compared to ion trap MS. The difference is likely a consequence of ion losses over
15 the ~ 1 m ion transfer path between the mass analyzers of the hybrid LTQ/FT-ICR MS instrument (M. C. Soule, personal communication, 2011). Automatic gain control was used to consistently fill the linear ion trap with the same number of ions ($n = 1 \times 10^6$) for each acquisition and to avoid space charge effects from over-filling the mass analyzer.

20 Tandem mass analysis (MS/MS) of selected precursor ions was performed within the FT-ICR mass analyzer using infrared multiphoton dissociation (IRMPD). Target precursor ions were isolated in the linear ion trap with an isolation width of 2 Da and then were transferred to the FT-ICR MS. The isolated ions were irradiated by the IRMPD light source with a normalized collision energy level of 100 % over $300\ \mu\text{s}$. The MS/MS
25 mass spectra were measured with a resolving power of 200 000 and 50 transients were acquired to produce product ion mass spectra.

Characterization of limonene ozonolysis SOA

S. Kundu et al.

Title Page

Abstract

Introduction

Conclusions

References

Tables

Figures

◀

▶

◀

▶

Back

Close

Full Screen / Esc

Printer-friendly Version

Interactive Discussion



2.3 Molecular formula assignment and quality control

Approximately 200 individual time domain transients were co-added with Sierra Analyt-
ics Composer software (Mazzoleni et al., 2010). Co-addition of numerous time domain
transients prior to Fourier transformation improves the signal-to-noise ratio (Kujawin-
ski et al., 2002) and the signal reproducibility (Soule et al., 2010). Several high relative
abundance SOA components were used as internal recalibrants (Sleighter et al., 2008;
Putman et al., 2011) to improve analyte mass accuracy. A full list of internal recalibrants
is given in Table S1. The molecular formula calculator was set to allow up to 100 car-
bon, 200 hydrogen, and 20 oxygen atoms per molecular composition. Unequivocal
formula assignment is expected up to 1000 Da when only C, H and O are included
(Koch et al., 2005).

Soule et al. (2010) have shown that ion detection and detector response of the ion
intensities in the ESI FT-ICR mass spectra are somewhat variable between replicate
analyses. Reproducibility is improved with the co-addition of 200 transients at a resolv-
ing power of 400 000. To further refine the list of ions, the common ions from replicate
analyses (SOA sample at 0% RH) and the analyses of two experiments with nearly
identical parameters were compared. More than 80% of the ions were common be-
tween replicate analyses of the sample and more than 85% of the ions were common
between the two experimental SOA samples generated at 0 and 4% relative humidity.
The comparison is shown in Figs. S1 and S2. A full list of the retained molecular for-
mulas is given Table S1. About 20% ions are common between blanks and aerosol
samples. Blank subtraction was not applied because the intensity in the blank sample
was less than 6% of that in the experimental SOA samples. The lower intensity of
common ions suggests they resulted from carry-over within the electrospray ionization
source.

Characterization of limonene ozonolysis SOA

S. Kundu et al.

Title Page

Abstract

Introduction

Conclusions

References

Tables

Figures

◀

▶

◀

▶

Back

Close

Full Screen / Esc

Printer-friendly Version

Interactive Discussion



3 Results and discussion

3.1 General characteristics of the SOA mass spectra

Approximately 1200 monoisotopic molecular formulas were identified in limonene ozonolysis SOA samples. Molecular formulas containing ^{13}C were identified and corresponded to molecular formulas providing an intrinsic validation of formula assignment (Schaub et al., 2005). The high number of molecular formulas identified in this study is associated with an increased sensitivity of the LTQ FT Ultra (Thermo Scientific) and the co-addition of ~ 200 transients (Kujawinski et al., 2002). The limonene ozonolysis SOA mass spectra has four prominent clusters of high relative abundance ions. Here we refer to these clusters as groups: Group I ($140 < m/z < 300$), Group II ($300 < m/z < 500$), Group III ($500 < m/z < 700$) and Group IV ($700 < m/z < 850$) (Fig. S3). This type of clustering of high relative abundance ions was previously observed in the soft ionization mass spectra of SOA from limonene ozonolysis and other terpene ozonolysis (Reinhardt et al., 2007; Tolocka et al., 2006; Walser et al., 2008). Previous studies have labeled them as monomers, dimers, trimers and tetramers. Mass differences between the ions within clusters are associated with the exact masses of CH_2 and O. Similar mass differences were observed in the mass spectra of SOA from limonene and α -pinene ozonolysis (Tolocka et al., 2004; Walser et al., 2008; Bateman et al., 2009).

3.2 Building units of high MW organic compounds

Consistent with previous studies (Heaton et al., 2007; Tolocka et al., 2004), Group I ($140 < m/z < 300$) compounds are considered to be the building units of high MW SOA. Group I includes 74 identified molecular formulas with relative abundances $>1\%$ (Fig. 1). The highest relative abundance ions are at the nominal masses of m/z 185 and 245, followed by nominal masses of m/z 261, 231, 215, 217, 171, 217, 199 and 247. Note that the relative abundances in the negative ion mass spectra might be influenced

Characterization of limonene ozonolysis SOA

S. Kundu et al.

Title Page

Abstract

Introduction

Conclusions

References

Tables

Figures

◀

▶

◀

▶

Back

Close

Full Screen / Esc

Printer-friendly Version

Interactive Discussion



by the ionization efficiency of analytes. A number of CH₂, O and CH₂O homologous series of compounds were observed. The chemical characteristics (O:C ratios, H:C ratios, DBE and OM:OC ratios) of this group are described in Table 1.

The relative abundances of CH₂ homologous series with DBE values of 3 are dominant in the mass spectra of Group I (Fig. 1c). The formation of a CH₂ homologous series with a DBE of 3 is illustrated in Fig. 2. The alkoxy radical (I, C₁₀H₁₅O₃) resulting from the limonene ozonolysis converts to another alkoxy radical (II, C₁₀H₁₅O₄) with one more oxygen atom following the isomerization, oxygen addition and RO₂ radical reactions (Walser et al., 2008). These three steps are collectively defined as oxygen-increasing-reactions. If the oxygen-increasing-reactions are repeated on this radical (II), alkoxy radicals with more oxygen, such as those labeled III (C₉H₁₃O₈), IV (C₁₀H₁₅O₈), V (C₉H₁₃O₆), and VI (C₁₀H₁₅O₆) in Fig. 2, can be produced. Alkoxy radicals such as that labeled as III and IV can be cleaved at the α -position of the alkoxy radical to form alkyl radicals with lower carbon numbers, which may form alkoxy radicals due to their reactions with O₂ and RO₂. Due to the subsequent RO₂ radical reactions on these alkoxy radicals, neutral molecules are formed including C₇H₁₀O₆, C₈H₁₂O₆, C₉H₁₄O₆ and C₁₀H₁₆O₆. They constitute the homologous series C₇H₁₀O₆ (CH₂)₀₋₅ (Fig. 1c).

Some of the components in the above mentioned homologous series contain 11 and 12 carbon atoms. One of these, C₁₁H₁₈O₆ corresponding to m/z 245, is the most prominent ion in the mass spectra (Fig. S3). These types of low MW secondary compounds are likely formed by the reactive uptake of gas-phase carbonyls (e.g., formaldehyde, acetaldehyde, acetone, glyoxal, methylglyoxal, etc.) generated from limonene ozonolysis (see Fig. 2b) (Jaoui et al., 2003; Lee et al., 2006). This conclusion is consistent with the observation of the prominence of the formaldehyde (CH₂O) homologous series (Fig. 1). Heaton et al. (2009) also suggested formaldehyde, acetaldehyde, and methylglyoxal as possible candidates for the growth of SOA in α - and β -pinene ozonolysis SOA. SOA growth by the uptake of gas-phase carbonyls has been demonstrated in both experimental (Jang and Kamens, 2001; Kroll et al., 2005) and theoretical studies

Characterization of limonene ozonolysis SOA

S. Kundu et al.

Title Page

Abstract

Introduction

Conclusions

References

Tables

Figures

◀

▶

◀

▶

Back

Close

Full Screen / Esc

Printer-friendly Version

Interactive Discussion



(Barsanti and Pankow, 2004, 2005). The experiment in our study was done without seed aerosols. However, the organic acids produced from monoterpene oxidation could provide the necessary acidity for catalytic reactions of gas-phase carbonyls onto generated organic aerosols (Gao et al., 2004). Reactive absorption of carbonyl compounds will be further evaluated by the fragmentation analysis in Sect. 3.4.

The relative abundances of the O homologous series with DBE values of 3 are the most prominent in the mass spectra (Fig. 1h). The formation of an O homologous series with DBE values of 3 is illustrated in Fig. 3. Alkyl radical (XI, $C_9H_{13}O_2$) could be produced by the α -cleavage of alkoxy radicals resulting from limonene ozonolysis (Walser et al., 2008). This alkyl radical is converted to another alkyl radical (XIII, $C_9H_{13}O_3$) with one more oxygen atom following oxygen-increasing-reactions (O_2 addition \rightarrow reactions with RO_2 radicals \rightarrow isomerization). If the oxygen-increasing-reactions are repeated on the alkyl radical (XIII, $C_9H_{13}O_3$), alkoxy radicals including XIV ($C_9H_{13}O_4$), XV ($C_9H_{13}O_5$), XVI ($C_9H_{13}O_6$) and XVII ($C_9H_{13}O_7$) are produced. These radicals react with RO_2 to form $C_9H_{14}O_4$, $C_9H_{14}O_5$, $C_9H_{14}O_6$ and $C_9H_{14}O_7$. The $C_9H_{14}O_3$ can be produced by the reactions of alkoxy radicals (XII, $C_9H_{13}O_3$) with RO_2 radicals. Together, they form the homologous series of $C_9H_{14}O_{3-7}$.

The formation processes for homologous series of compounds with DBE values of 4 are similar to that of homologous series of compounds with DBE values of 3, as shown in Fig. S4. Homologous series of compounds with DBE values of 2 are observed with significant relative abundances (Fig. 1b, g and l). The hydration of carbonyl group could reduce the DBE values from 3 to 2. While some hydration reactions may occur in the reaction chamber, hydration reactions are most likely to occur during the aqueous extraction in this study. Similarly, Yasmeen et al. (2010) reported evidence for the acid-catalyzed hydration of methylglyoxal in dark model cloud water reactions.

3.3 Characteristics and formation of high MW SOA compounds

Similar to the low MW compounds, CH_2 and O homologous were observed in each group of the high MW compounds. The chemical characteristics of the high MW

Characterization of limonene ozonolysis SOA

S. Kundu et al.

Title Page

Abstract

Introduction

Conclusions

References

Tables

Figures

◀

▶

◀

▶

Back

Close

Full Screen / Esc

Printer-friendly Version

Interactive Discussion



compounds in Groups II, III and IV are described in Table 1.

The most prominent DBE values observed in Group I, Group II and Group III are 3, 5 and 7 (Fig. 4). Similarly, the prominent difference of DBE values between groups is 2. Similar DBE increments of 2 were observed in limonene ozonolysis SOA by Bateman et al., 2009. They interpreted it to be associated with a predominance for Criegee and hemi-acetal reaction channels over the condensation reaction channels. As they demonstrated, the increment of 2 DBE occurs in Criegee and hemiacetal reactions (Fig. S5) and increment of 3 DBE occurs in condensation reactions (aldol and esterification) (Fig. S6). However, the increments of DBE 2 may also occur in the hydroperoxide reaction channel (Fig. S5); so, this reaction channel may also be responsible for the predominance of the DBE increments observed in limonene SOA. An exception to this is an increase of 3 DBE in some Criegee radical reactions and 2 DBE in some aldol condensation reactions (see Figs. S5 and S6). Thus, the higher significance of the hydroperoxide, Criegee and hemi-acetal reactions compared to the condensation reaction channels needs further validation. Fragmentation analyses of selected peaks in Sect. 3.4 are used as an additional interpretive tool to determine the relative importance of the reaction channels.

Elemental ratios of hydrogen and oxygen to carbon are useful for classification of complex organic compounds and for evaluating the formation processes of high MW SOA. The van Krevelen diagram, a plot of H:C vs. O:C, for limonene SOA is shown in Fig. 5. A significant fraction of high abundance compounds was observed with O:C ratios of approximately 0.4–0.7 and with H:C ratios <1.5. They are associated with aliphatic high MW compounds with multifunctional groups. The average O:C ratio decreases from Group I (0.59 ± 0.18) to Group II (0.51 ± 0.13) compounds (Fig. 5b). There is no significant differences between the O:C and H:C ratios of Group III (0.49 ± 0.09 ; 1.6 ± 0.11) and those of Group II compounds (0.51 ± 0.13 ; 1.53 ± 0.16). The observed O:C ratio decrease with increasing MW differs from the interpretation of the observed O:C ratios from aerosol mass spectrometry analysis of ambient atmospheric aerosols at many locations in the Northern Hemisphere (Jimenez et al., 2009).

Characterization of limonene ozonolysis SOA

S. Kundu et al.

Title Page

Abstract

Introduction

Conclusions

References

Tables

Figures

◀

▶

◀

▶

Back

Close

Full Screen / Esc

Printer-friendly Version

Interactive Discussion



For example, the O:C ratios of low-volatility oxygenated organic aerosol (LV-OOA), representing oligomeric and other high MW organic aerosols, are higher than those of semi-volatile OOA (SV-OOA), representing comparatively fresh and low MW organic aerosols. This suggests that O:C ratios observed using aerosol mass spectrometry are more influenced by the low MW compounds. The decrease in O:C ratios from Group I to Group II was interpreted by Reinhardt et al. (2007) as an elimination of H₂O during the formation of high MW SOA from α -pinene ozonolysis following condensation reactions. However if water is eliminated as proposed, it is also expected that the H:C ratio will also decrease from Group I (1.5 ± 0.20) to Group II (1.5 ± 0.16). We did not observe a change in H:C ratios which indicates less significance for the condensation reaction channels. These observations and the DBE trends suggest a higher significance for the hydroperoxide, Crigee and hemi-acetal reaction channels. Additional evidence will be provided by the fragmentation analysis of the selected ions presented in Sect. 3.4.

As discussed, SOA components observed in Group II and Group III are expected to represent combinations of hydroperoxides, Criegee radicals and Group I compounds. Reaction matrixes were created for several different reaction channels to identify the formation processes of the high MW compounds. They included nine limonene derived hydroperoxides (Heaton et al., 2007), three limonene derived Criegee radicals (Docherty et al., 2004) and high abundant (RA > 1%) neutral molecules from Group I analytes. Hydroperoxides and Criegee radicals are expected to react with a neutral molecule leading to the formation of the high MW SOA components. Reactions may occur between alcohol and carbonyl functional groups in the hemi-acetal reaction channel. Alcohols may also react with carboxylic acids by the esterification reaction channel. Carbonyl containing compounds react together with the elimination of a water molecule in the aldol condensation reaction channel. The schematics of these reaction processes are shown in Figs. S5 and S6. Using this approach, 136 Group II compounds and 90 Group III compounds were matched to the products of the hydroperoxide reaction channel. The Criegee reaction channel matched 90 Group II compounds and

Characterization of limonene ozonolysis SOA

S. Kundu et al.

Title Page

Abstract

Introduction

Conclusions

References

Tables

Figures

◀

▶

◀

▶

Back

Close

Full Screen / Esc

Printer-friendly Version

Interactive Discussion



68 Group III compounds. Reaction products of the hemi-acetal channel corresponded to 172 Group II compounds and 88 Group III compounds. Products of the condensation reaction channels matched 164 Group II compounds and 87 Group III compounds. Results of the 50 most abundant Group II compounds are shown in Fig. 6. They show that most of the high MW compounds are formed by multiple reaction pathways and a higher matching probability was obtained using the hemi-acetal and condensation reaction pathways than using the Criegee and hydroperoxide reaction pathways. Similar results were also observed for Group III compounds (see Table S2). The reaction matrix analysis suggests that none of the presented channels can be excluded as possible formation mechanisms for the formation of high MW SOA.

3.4 Structural elucidation of selected ions

Fragmentation analysis was done for a better understanding of the molecular composition and the formation processes of high MW compounds. Fragmentation of isobaric ions within 2 Da was performed on the abundant nominal masses of m/z 245, 401 and 587. Due to limitation in the isolation of precursor ions, the fragmentation analysis cannot be done on singular analyte. It is assumed that a majority of the product ions were generated from the peaks with the greatest intensities in the isolation range.

The product ion mass spectrum for m/z 245 ± 2 fragmentation is shown in Fig. 7. The dominant precursor ion is m/z 245.1032 ($C_{11}H_{18}O_6$) and there are 9 less abundant isobaric ions at m/z 245 (inset panel). This compound was previously proposed to be formed by the reactive absorption of vapor phase carbonyl as shown in Fig. 2b. The expected major fragments of this compound and its structural isomers were observed in the product ion spectrum (Fig. 7). Fragments in the high mass range ($m/z \geq 165$) are related to the elimination of neutral molecules (i.e. H_2O and CO_2) from the precursor ions. They include peaks at m/z 165, 183, 201, 209, and 227. Examples of these product ions are shown in the lower panel (a). Fragmentation can occur at the β -carbon relative to the carboxyl or carbonyl groups via the McLafferty rearrangement in the structural isomers (lower panels, b, c and d); resulting product ions at m/z 59, 73,

Characterization of limonene ozonolysis SOA

S. Kundu et al.

Title Page

Abstract

Introduction

Conclusions

References

Tables

Figures

◀

▶

◀

▶

Back

Close

Full Screen / Esc

Printer-friendly Version

Interactive Discussion



75, 89, 105, 139, 155, 171, 169 and 185. Fragmentation at the α -position relative to the OH group in structural isomer (lower panel, e) can produce ions at m/z 157, 87, 99, 117 and 127. Evidence for the existence of a few structural isomers for the precursor ions is observed in the mass spectrum. Similar types of neutral molecule eliminations may explain the other dominant ion at m/z 185. Its mass spectrum and fragmentation processes are provided in Fig. S7a.

As indicated by the reaction matrix, several combinations of building units following different reaction channels were identified for m/z 401.1817 ($C_{19}H_{30}O_9$) and 401.2179 ($C_{20}H_{34}O_8$). See the inset in Fig. 7a. These results indicate that the peak at m/z 401.1817 and 401.2179 can be formed by all the mentioned reaction pathways. Fragmentation analysis was done to evaluate them. The product ion mass spectrum for fragments at nominal m/z 401 is shown in Fig. 7a. The product ions are assumed to be predominantly from the most prominent ions 401.1817 and 401.219. Note there are 13 isobaric peaks at m/z 401. The building blocks (shown in the figure inset) associated with hydroperoxide, Criegee and hemiacetal reaction channels can explain most of the prominent peaks between m/z 143 and 245. The m/z of the building units is ≥ 230 for the majority of the combinations following the condensation (aldol and esterification) reaction channels and they are not observed as prominent product ions. Similar results were also obtained for other prominent ions at m/z 357 ± 2 , 387 ± 2 , and 417 ± 2 . Their product ion mass spectra are shown in Fig. S7. The results further support the importance of hydroperoxide, Criegee and hemiacetal reactions over condensation reactions for the formation of high MW Group II compounds. The prominent fragments at the high m/z region are 303, 321, 339, 365 and 383. They are related with neutral molecule elimination (i.e. H_2O , CO_2 and their combinations) from the precursors. The product ions $< m/z$ 140 are likely result of secondary fragmentation of building units relative to m/z 401. Typical fragmentation processes of the building units of high MW organic compounds have been shown previously in Fig. 7.

For the dominant isobaric ions at m/z 587.2343, 587.2708 and 587.3074 (formulas: $C_{27}H_{40}O_{14}$, $C_{28}H_{44}O_{13}$, $C_{29}H_{48}O_{12}$) in Fig. 8b, many combinations of building units

Characterization of limonene ozonolysis SOA

S. Kundu et al.

Title Page

Abstract

Introduction

Conclusions

References

Tables

Figures

◀

▶

◀

▶

Back

Close

Full Screen / Esc

Printer-friendly Version

Interactive Discussion



were observed following different reaction channels. They are shown in the inset. The molecular weight of at least one building unit is >230 in 80% of the potential combinations following condensation reactions. The product ions of these precursors are much less abundant in the mass spectrum. Similar results were also obtained from the fragmentation of the ions at m/z 541 (Fig. S7). These results further suggest greater importance of hydroperoxide, Criegee and hemi-acetal reactions in the high MW compound formation. The ions of the high m/z region at 569, 551 and 515 are associated with the elimination of neutral molecules (i.e. H_2O , CO_2). The ions in the middle m/z region including: m/z 401, 399, 385, 369, 355, 339, 327 and 315 are due to the loss of neutral building units including 186, 188, 202, 218, 232, 248, and 260, respectively, from the precursor ions. Most of the prominent peaks in the middle m/z region of 143–300 are related to the secondary fragmentation of the participating building units of the high MW compounds. The ions at lower m/z values might have resulted from the characteristic fragmentation processes of the building units of high MW compounds as shown in Fig. 7.

Product ions in Fig. 8a are associated with a Group II precursor and product ions in Fig. 8b are associated with a Group III precursor. The m/z region of 300–450 was shown only in the product ion spectra of Group III compounds. This suggests the presence of an additional building unit in the molecules of Group III compounds. Most of the building units in the m/z of 150–300 are common in the spectra of Group II and Group III compounds; however, their intensities are different. These results suggest the participation of different amounts of the building units in high MW compound formation.

4 Conclusions

Using ultrahigh-resolution Fourier transform ion cyclotron resonance mass spectrometry (FT-ICR MS), 1197 molecular formulas were identified in the SOA of limonene ozonolysis. Four characteristic ion clusters with high relative abundances were observed. The mechanistic reaction pathways for the formation of CH_2 and O

Characterization of limonene ozonolysis SOA

S. Kundu et al.

Title Page

Abstract

Introduction

Conclusions

References

Tables

Figures

◀

▶

◀

▶

Back

Close

Full Screen / Esc

Printer-friendly Version

Interactive Discussion



**Characterization of
limonene ozonolysis
SOA**

S. Kundu et al.

Title Page

Abstract

Introduction

Conclusions

References

Tables

Figures

◀

▶

◀

▶

Back

Close

Full Screen / Esc

Printer-friendly Version

Interactive Discussion



homologous series in the low MW compounds ($140 < m/z < 300$) were explained by reactions involving Criegee radicals, alkyl peroxy radicals and alkoxy radicals. The presence of formaldehyde (CH_2O) homologous series and the fragmentation analysis of selected ions in Group 1 ($140 < m/z < 300$) provides evidence for aerosol formation by the reactive uptake of vapor phase carbonyls. The DBE changes of 2 from Group I to Group II and Group II to Group III indicate a predominance of non-condensation reaction pathways (hydroperoxide, Criegee and hemi-acetal) over condensation (aldol and esterification) reaction pathways. The decreasing trends O:C ratios between group of compounds suggest the importance of condensation reaction pathways over non-condensation reaction pathways. Note that O:C ratios are decreased as a result of elimination of water in the condensation reactions. The highest frequency of matches was found for the hemi-acetal and condensation (aldol and esterification) reaction pathways. We observed that the interpretation of the molecular DBE values and the elemental ratios may sometimes result in ambiguous conclusions about the formation processes of high MW SOA ($m/z > 300$). It is also difficult to interpret the formation processes of high MW compounds using a comprehensive reaction matrix since a majority of the individual high MW compounds can be produced via several different reaction channels. In this work, we presented an integrated approach to elucidate high MW SOA formation processes using the DBE, elemental ratios (O:C and H:C ratios), reaction matrix and fragmentation analysis. This comprehensive approach indicates the importance of non-condensation reactions (hydroperoxide, Criegee and hemiacetal) over the condensation (aldol and esterification) reactions for the high MW compound ($m/z > 300$) formation. Among the non-condensation reactions, hemi-acetal reactions are most dominant followed by hydroperoxide and Criegee reactions. The results indicate that most of the high MW compounds are accretions of multiple building units which cannot be explained by a single building block approach.

Supplementary material related to this article is available online at:
[http://www.atmos-chem-phys-discuss.net/12/2167/2012/
acpd-12-2167-2012-supplement.zip](http://www.atmos-chem-phys-discuss.net/12/2167/2012/acpd-12-2167-2012-supplement.zip).

Acknowledgements. Major research funding for this work was provided by the Los Alamos National Laboratory, Laboratory Directed Research and Development program. The authors thank Melissa Soule and Elizabeth Kujawinski of the Wood Hole Oceanographic Institution Mass Spectrometry Facility for instrument time and assistance with data acquisition. We also thank Dr. Giuseppe Petrucci of University of Vermont for the helpful discussions. Shuvashish Kundu thanks David and Valeria Pruetz for fellowship support via the Department of Chemistry at Michigan Tech.

References

- Barsanti, K. C. and Pankow, J. F.: Thermodynamics of the formation of atmospheric organic particulate matter by accretion reactions – part 1: aldehydes and ketones, *Atmos. Environ.*, 38, 4371–4382, 2004.
- Barsanti, K. C. and Pankow, J. F.: Thermodynamics of the formation of atmospheric organic particulate matter by accretion reactions: Part 2: Dialdehydes, methylglyoxal, and diketones, *Atmos. Environ.*, 39, 6597–6607, 2005.
- Bateman, A. P., Nizkorodov, S. A., Laskin, J., and Laskin, A.: Time-resolved molecular characterization of limonene/ozone aerosol using high-resolution electrospray ionization mass spectrometry, *Phys. Chem. Chem. Phys.*, 11, 7931–7942, 2009.
- Docherty, K. S., Kumboonlert, K., Lee, I. J., and Ziemann, P. J.: Gas chromatography of trimethylsilyl derivatives of α -methoxyalkyl hydroperoxides formed in alkene- O_3 reactions, *J. Chromatogr. A*, 1029, 205–215, 2004.
- Docherty, K. S., Wilbur, W., Lim, Y. B., and Ziemann, P. J.: Contributions of organic peroxides to secondary aerosol formed from reactions of monoterpenes with O_3 , *Environ. Sci. Technol.*, 39, 4049–4059, 2005.
- Fuzzi, S., Andreae, M. O., Huebert, B. J., Kulmala, M., Bond, T. C., Boy, M., Doherty, S. J., Guenther, A., Kanakidou, M., Kawamura, K., Kerminen, V.-M., Lohmann, U., Russell, L. M.,

ACPD

12, 2167–2197, 2012

Characterization of limonene ozonolysis SOA

S. Kundu et al.

Title Page

Abstract

Introduction

Conclusions

References

Tables

Figures

◀

▶

◀

▶

Back

Close

Full Screen / Esc

Printer-friendly Version

Interactive Discussion



**Characterization of
limonene ozonolysis
SOA**

S. Kundu et al.

Title Page

Abstract

Introduction

Conclusions

References

Tables

Figures

◀

▶

◀

▶

Back

Close

Full Screen / Esc

Printer-friendly Version

Interactive Discussion



and Pschl, U.: Critical assessment of the current state of scientific knowledge, terminology, and research needs concerning the role of organic aerosols in the atmosphere, climate, and global change, *Atmos. Chem. Phys.*, 6, 2017–2038, doi:10.5194/acp-6-2017-2006, 2006.

Gao, S., Ng, A. L., Keywood, M., Varutbangkul, V., Bahreini, R., Nenes, A., He, J. W., Yoo, K. Y., Beauchamp, J. L., Hodyss, R. P., Flagan, R. C., Seinfeld, J. H.: Particle Phase Acidity and Oligomer Formation in Secondary Organic Aerosol, *Environ. Sci. Technol.*, 38, 1428–1434, 2004.

Geddes, S., Nichols, B., Flemer Jr., S., Eisenhauer, J., Zahardis, J., Petrucci, G. A.: Near-infrared laser desorption/ionization aerosol mass spectrometry for investigating organic aerosols under low loading conditions, *Anal. Chem.*, 82, 7915–7923, 2010.

Hallquist, M., Wenger, J. C., Baltensperger, U., Rudich, Y., Simpson, D., Claeys, M., Dommen, J., Donahue, N. M., George, C., Goldstein, A. H., Hamilton, J. F., Herrmann, H., Hoffmann, T., Iinuma, Y., Jang, M., Jenkin, M. E., Jimenez, J. L., Kiendler-Scharr, A., Maenhaut, W., McFiggans, G., Mentel, Th. F., Monod, A., Prévôt, A. S. H., Seinfeld, J. H., Surratt, J. D., Szmigielski, R., and Wildt, J.: The formation, properties and impact of secondary organic aerosol: current and emerging issues, *Atmos. Chem. Phys.*, 9, 5155–5236, doi:10.5194/acp-9-5155-2009, 2009.

Hamilton, J. F., Lewis, A. C., Reynolds, J. C., Carpenter, L. J., and Lubben, A.: Investigating the composition of organic aerosol resulting from cyclohexene ozonolysis: low molecular weight and heterogeneous reaction products, *Atmos. Chem. Phys.*, 6, 4973–4984, doi:10.5194/acp-6-4973-2006, 2006.

Heaton, K. J., Dreyfus, M. A., Wang, S., and Johnston, M. V.: Oligomers in the early stage of biogenic secondary organic aerosol formation and growth, *Environ. Sci. Technol.*, 41, 6129–6136, doi:10.1021/es070314n, 2007.

Heaton, K. J., Slighter, R. L., Hatcher, P. G., Hall, W. A. I., and Johnston, M. V.: Composition domains in monoterpene secondary organic aerosol, *Environ. Sci. Technol.*, 43, 7797–7802, 2009.

Iinuma, Y., Böge, O., Gnauk, T., and Herrmann, H.: Aerosol-chamber study of the α -pinene/ O_3 reaction: Influence of particle acidity on aerosol yields and products, *Atmos. Environ.*, 38, 761–773, 2004.

Jang, M. and Kamens, R. M.: Atmospheric Secondary Aerosol Formation by Heterogeneous Reactions of Aldehydes in the Presence of a Sulfuric Acid Aerosol Catalyst, *Environ. Sci. Technol.*, 35, 4758–4766, 2001.

Jimenez, J. L., Canagaratna, M. R., Donahue, N. M., Prevot, A. S. H., Zhang, Q., Kroll, J. H., DeCarlo, P. F., Allan, J. D., Coe, H., Ng, N. L., Aiken, A. C., Docherty, K. S., Ulbrich, I. M., Grieshop, A. P., Robinson, A. L., Duplissy, J., Smith, J. D., Wilson, K. R., Lanz, V. A., Hueglin, C., Sun, Y. L., Tian, J., Laaksonen, A., Raatikainen, T., Rautiainen, J., Vaattovaara, P., Ehn, M., Kulmala, M., Tomlinson, J. M., Collins, D. R., Cubison, M. J., Dunlea, E. J., Huffman, J. A., Onasch, T. B., Alfarra, M. R., Williams, P. I., Bower, K., Kondo, Y., Schneider, J., Drewnick, F., Borrmann, S., Weimer, S., Demerjian, K., Salcedo, D., Cottrell, L., Griffin, R., Takami, A., Miyoshi, T., Hatakeyama, S., Shimojo, A., Sun, J. Y., Zhang, Y. M., Dzepina, K., Kimmel, J. R., Sueper, D., Jayne, J. T., Herndon, S. C., Trimborn, A. M., Williams, L. R., Wood, E. C., Middlebrook, A. M., Kolb, C. E., Baltensperger, U., and Worsnop, D. R.: Evolution of organic aerosols in the atmosphere, *Science*, 326, 1525–1529, 2009.

Jonsson, Å. M., Hallquist, M., and Ljungström, E.: The effect of temperature and water on secondary organic aerosol formation from ozonolysis of limonene, Δ^3 -carene and α -pinene, *Atmos. Chem. Phys.*, 8, 6541–6549, doi:10.5194/acp-8-6541-2008, 2008.

Kalberer, M., Paulsen, D., Sax, M., Steinbacher, M., Dommen, J., Fisseha, R., and Prévôt, A. S. H., Frankevich, V., Zenobi, R., and Baltensperger, U.: Identification of polymers as major components of atmospheric organic aerosols, *Science*, 303, 1659–1662, 2004.

Kanakidou, M., Seinfeld, J. H., Pandis, S. N., Barnes, I., Dentener, F. J., Facchini, M. C., Van Dingenen, R., Ervens, B., Nenes, A., Nielsen, C. J., Swietlicki, E., Putaud, J. P., Balkanski, Y., Fuzzi, S., Horth, J., Moortgat, G. K., Winterhalter, R., Myhre, C. E. L., Tsigaridis, K., Vignati, E., Stephanou, E. G., and Wilson, J.: Organic aerosol and global climate modelling: a review, *Atmos. Chem. Phys.*, 5, 1053–1123, doi:10.5194/acp-5-1053-2005, 2005.

Koch, B. P., Witt, M., Engbrodt, R., Dittmar, T., and Kattner, G.: Molecular formulae of marine and terrigenous dissolved organic matter detected by electrospray ionization Fourier transform ion cyclotron resonance mass spectrometry, *Geochim. Cosmochim. Ac.*, 69, 3299–3308, 2005.

Kroll, J. H., Ng, N. L., Murphy, S. M., Varutbangkul, V., Flagan, R. C., and Seinfeld, J. H.: Chamber studies of secondary organic aerosol growth by reactive uptake of simple carbonyl compounds, *J. Geophys. Res.-Atmos.*, 110, D23207, doi:10.1029/2005JD006004, 2005.

Kujawinski, E. B., Freitas, M. A., Zang, X., Hatcher, P. G., Green-Church, K. B., and Jones, R. B.: The application of electrospray ionization mass spectrometry (ESI-MS) to the structural characterization of natural organic matter, *Org. Geochem.*, 33, 171–180, 2002.

Lee, A., Goldstein, A. H., Kroll, J. H., Ng, N. L., Varutbangkul, V., Flagan, R. C., and Seinfeld, J.

ACPD

12, 2167–2197, 2012

Characterization of limonene ozonolysis SOA

S. Kundu et al.

Title Page

Abstract

Introduction

Conclusions

References

Tables

Figures

◀

▶

◀

▶

Back

Close

Full Screen / Esc

Printer-friendly Version

Interactive Discussion



**Characterization of
limonene ozonolysis
SOA**

S. Kundu et al.

Title Page

Abstract

Introduction

Conclusions

References

Tables

Figures

◀

▶

◀

▶

Back

Close

Full Screen / Esc

Printer-friendly Version

Interactive Discussion



H.: Gas-phase products and secondary aerosol yields from the photooxidation of 16 different terpenes, *J. Geophysical Research*, 111, D17305, doi:10.1029/2006JD007050, 2006.

Leungsakul, S., Jaoui, M., and Kamens, R. M.: Kinetic mechanism for predicting secondary organic aerosol formation from the reaction of d-limonene with ozone, *Environ. Sci. Technol.*, 39, 9583–9594, doi:10.1021/es0492687, 2005.

Liao, H., Henze, D. K., Seinfeld, J. H., Wu, S., and Mickley, L. J.: Biogenic secondary organic aerosol over the United States: Comparison of climatological simulations with observations, *J. Geophys. Research*, 112, D06201, doi:10.1029/2006JD007813, 2007.

Mazzoleni, L. R., Ehrmann, B. M., Shen, X., Marshall, A. G., and Collett, J. L.: Water-soluble atmospheric organic matter in fog: Exact masses and chemical formula identification by ultrahigh-resolution Fourier transform ion cyclotron resonance mass spectrometry, *Environ. Sci. Technol.*, 44, 3690–3697, doi:10.1021/es903409k, 2010.

Putman, A., Offenberg, J. H., Rebeka, F., Kundu, S., Rahn, T., and Mazzoleni, L. R.: Ultrahigh-resolution FT-ICR mass spectrometry of α -pinene ozonolysis SOA, *Atmos. Environ.*, 46, 164–172, doi:10.1016/j.atmosenv.2011.10.003, 2011.

Reinhardt, A., Emmenegger, C., Gerrits, B., Panse, C., Dommen, J., Baltensperger, U., Zenobi, R., and Kalberer, M.: Ultrahigh mass resolution and accurate mass measurements as a tool to characterize oligomers in secondary organic aerosols, *Anal. Chem.*, 79, 4074–4082, doi:10.1021/ac062425v, 2007.

Salma, I., Ocskay, R., and Láng, G. G.: Properties of atmospheric humic-like substances – water system, *Atmos. Chem. Phys.*, 8, 2243–2254, doi:10.5194/acp-8-2243-2008, 2008.

Schaub, T. M., Hendrickson, C. L., Quinn, J. P., Rodgers, R. P., and Marshall, A. G.: Instrumentation and method for ultrahigh resolution field desorption ionization Fourier transform ion cyclotron resonance mass spectrometry of nonpolar species, *Anal. Chem.*, 77, 1317–1324, 2005.

Sleighter, R. L., Liu, Z., Xue, J., and Hatcher, G. P.: Multivariate statistical approaches for the characterization of dissolved organic matter analyzed by ultrahigh resolution mass spectrometry, *Environ. Sci. Technol.*, 44, 7576–7582, 2010.

Soule, M. C., Longnecker, K., Giovannoni, S. J., and Kujawinski, E. B.: Impact of instrument and experiment parameters on reproducibility of ultrahigh resolution ESI FT-ICR mass spectra of natural organic matter, *Org. Geochem.*, 41, 725–733, 2010.

Stroud, C., Makar, P., Karl, T., Guenther, A., Geron, C., Turnipseed, A., Nemitz, E., Baker, B., Potosnak, M., and Fuentes, J. D.: Role of canopy-scale photochemistry in modifying

**Characterization of
limonene ozonolysis
SOA**

S. Kundu et al.

Title Page

Abstract

Introduction

Conclusions

References

Tables

Figures

◀

▶

◀

▶

Back

Close

Full Screen / Esc

Printer-friendly Version

Interactive Discussion



biogenic-atmosphere exchange of reactive terpene species: Results from the celtic field study, *J. Geophys. Res.*, 110, D17303, doi:10.1029/2005jd005775, 2005.

Surratt, J. D., Murphy, S. M., Kroll, J. H., Ng, N. L., Hildebrandt, L., Sorooshian, A., Szmigielski, R., Vermeylen, R., Maenhaut, W., Claeys, M., Flagan, R. C., and Seinfeld, J. H.: Chemical composition of secondary organic aerosol formed from the photooxidation of isoprene, *The Journal of Physical Chemistry A*, 110, 9665–9690, doi:10.1021/jp061734m, 2006.

Tolocka, M. P., Jang, M., Ginter, J. M., Cox, F. J., Kamens, R. M., and Johnston, M. V.: Formation of Oligomers in Secondary Organic Aerosol, *Environ. Sci. Technol.*, 38, 1428–1434, 2004.

Tolocka, M. P., Heaton, K. J., Dreyfus, M. A., Wang, S., Zordan, C. A., Saul, T. D., and Johnston, M. V.: Chemistry of Particle Inception and Growth during α -Pinene Ozonolysis, *Environ. Sci. Technol.*, 40, 1843–1848, 2006.

Walser, M. L., Desyaterik, Y., Laskin, J., Laskin, A., and Nizkorodov, S. A.: High-resolution mass spectrometric analysis of secondary organic aerosol produced by ozonation of limonene, *Phys. Chem. Chem. Phys.*, 10, 1009–1022, 2008.

Went, F. W.: Blue hazes in the atmosphere, *Nature*, 187, 641–643, 1960.

Yasmeen, F., Sauret, N., Gal, J.-F., Maria, P.-C., Massi, L., Maenhaut, W., and Claeys, M.: Characterization of oligomers from methylglyoxal under dark conditions: a pathway to produce secondary organic aerosol through cloud processing during nighttime, *Atmos. Chem. Phys.*, 10, 3803–3812, doi:10.5194/acp-10-3803-2010, 2010.

Ziemann, P. J.: Aerosol products, mechanisms, and kinetics of heterogeneous reactions of ozone with oleic acid in pure and mixed particles, *Faraday Discuss.*, 130, 469–490, doi:10.1039/B417502F, 2005.

Characterization of limonene ozonolysis SOA

S. Kundu et al.

Table 1. Chemical characteristics of the compound groups observed in the mass spectra.

| Compounds | O:C | | H:C | | DBE | | OM:OC | |
|-----------|---------|----------------|---------|----------------|-------|----------------|---------|----------------|
| | Range | Avg. \pm Sd. | Range | Avg. \pm Sd. | Range | Avg. \pm Sd. | Range | Avg. \pm Sd. |
| Group I | 0.3–1 | 0.6 \pm 0.2 | 1.1–2.0 | 1.5 \pm 0.2 | 1–7 | 3.5 \pm 1.3 | 1.5–2.4 | 1.9 \pm 0.2 |
| Group II | 0.3–0.9 | 0.5 \pm 0.1 | 1.2–1.9 | 1.5 \pm 0.2 | 2–9 | 5.3 \pm 1.4 | 1.5–2.3 | 1.8 \pm 0.2 |
| Group III | 0.3–0.8 | 0.5 \pm 0.1 | 1.3–1.8 | 1.6 \pm 0.1 | 4–10 | 7.0 \pm 1.6 | 1.5–2.1 | 1.8 \pm 0.1 |
| Group IV | 0.3–0.6 | 0.5 \pm 0.1 | 1.4–1.7 | 1.6 \pm 0.1 | 6–11 | 8.6 \pm 1.4 | 1.6–2.0 | 1.8 \pm 0.1 |

Title Page

Abstract

Introduction

Conclusions

References

Tables

Figures

◀

▶

◀

▶

Back

Close

Full Screen / Esc

Printer-friendly Version

Interactive Discussion



Characterization of limonene ozonolysis SOA

S. Kundu et al.

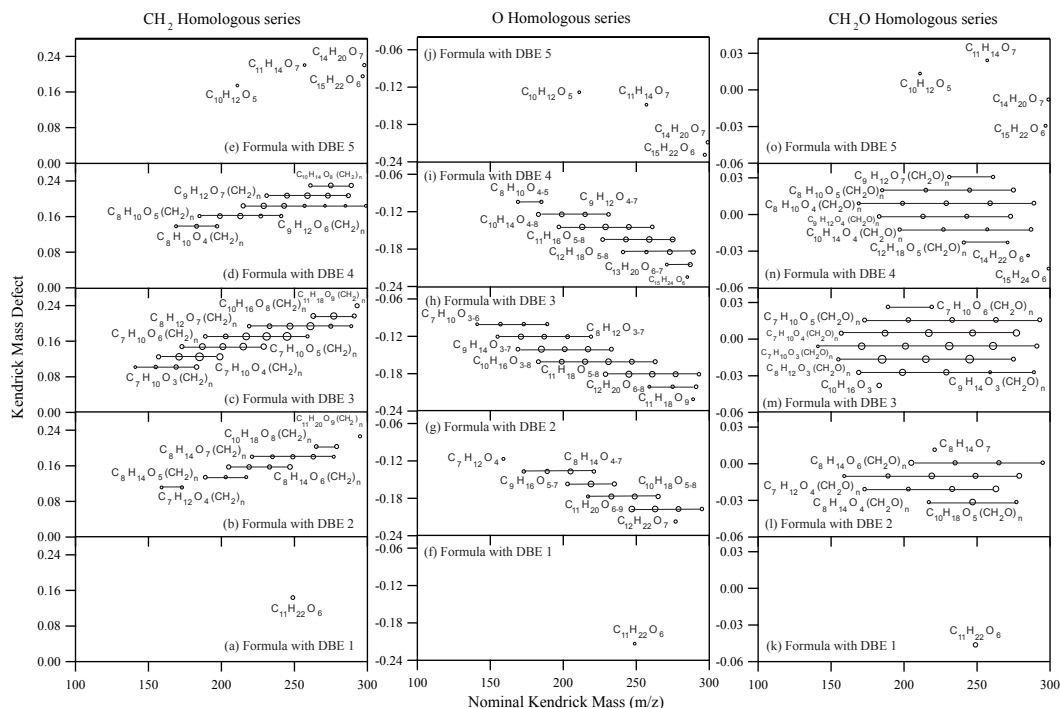


Fig. 1. CH_2 , O and CH_2O homologous series of negative ions with $\geq 1\%$ relative abundance for the mass range of $140 < m/z < 300$. Components of the homologous series fall onto the horizontal lines. Data points were scaled according to the logarithm of their measured relative abundances. The value of “ n ” starts from zero.

Title Page

Abstract

Introduction

Conclusions

References

Tables

Figures

◀

▶

◀

▶

Back

Close

Full Screen / Esc

Printer-friendly Version

Interactive Discussion



Characterization of limonene ozonolysis SOA

S. Kundu et al.

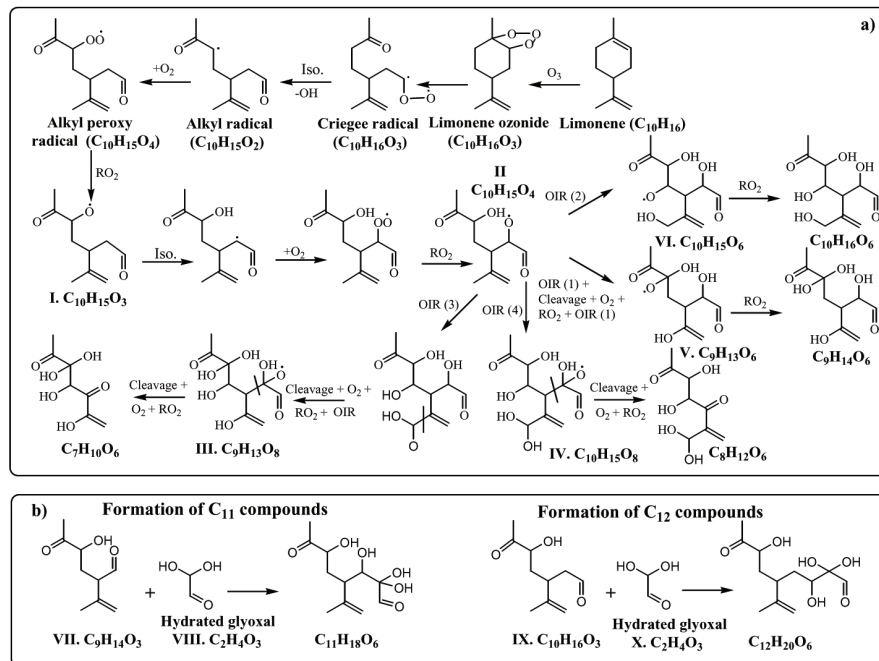


Fig. 2. Depiction of the potential formation mechanisms of CH_2 homologous series. **(a)** Alkoxy radical (I) resulting from the limonene ozonolysis which undergoes oxygen-increasing-reactions (OIR, isomerization $\rightarrow O_2 \rightarrow RO_2$) to become an alkoxy radical (II) with an additional oxygen atom. OIR sequence repeats to form alkoxy radicals labeled III, IV, V and VI. The number in the parenthesis beside “OIR” indicates the repetition of OIR sequence. These alkoxy radicals are converted to neutral molecules to form the homologous series. The schematics in **(b)** show organic aerosol formation for C_{11} - C_{12} compounds by the reactive uptake of a gas phase carbonyl (e.g., glyoxal).

Title Page

Abstract

Introduction

Conclusions

References

Tables

Figures

◀

▶

◀

▶

Back

Close

Full Screen / Esc

Printer-friendly Version

Interactive Discussion



Characterization of limonene ozonolysis SOA

S. Kundu et al.

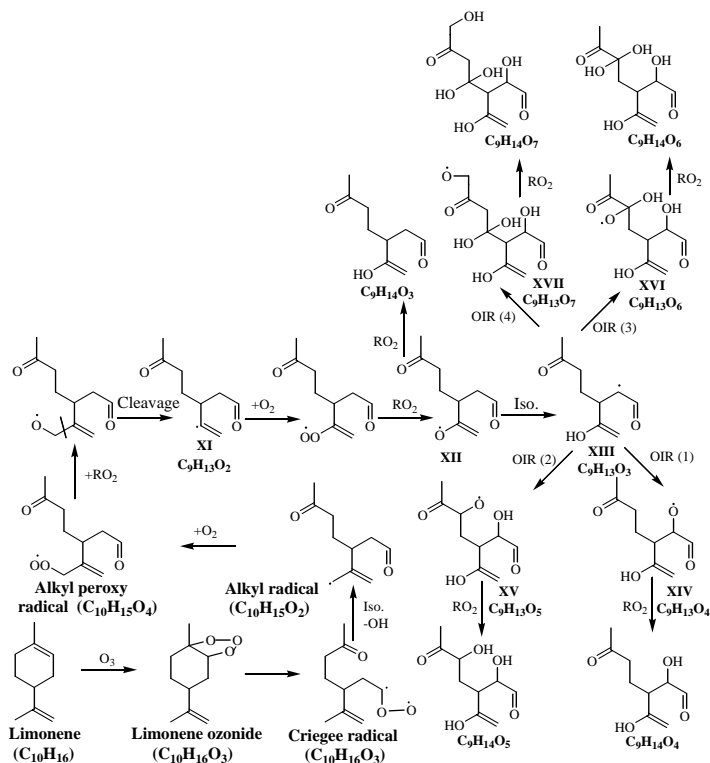


Fig. 3. Illustration depicting the formation of O homologous series. Alkoxy radical resulting from the limonene ozonolysis could convert to alkyl radical (XI) by cleavage. Oxygen-increasing-reactions (OIR, $O_2 \rightarrow RO_2 \rightarrow$ isomerization) produce an alkyl radical (XIII) with an additional oxygen atom. Further OIR sequences result in alkoxy radicals labeled as XIV, XV and XVI and XVII. They are transformed to neutral molecules by reactions with RO_2 and comprise the O homologous series.

Title Page

Abstract Introduction

Conclusions References

Tables Figures

◀ ▶

◀ ▶

Back Close

Full Screen / Esc

Printer-friendly Version

Interactive Discussion



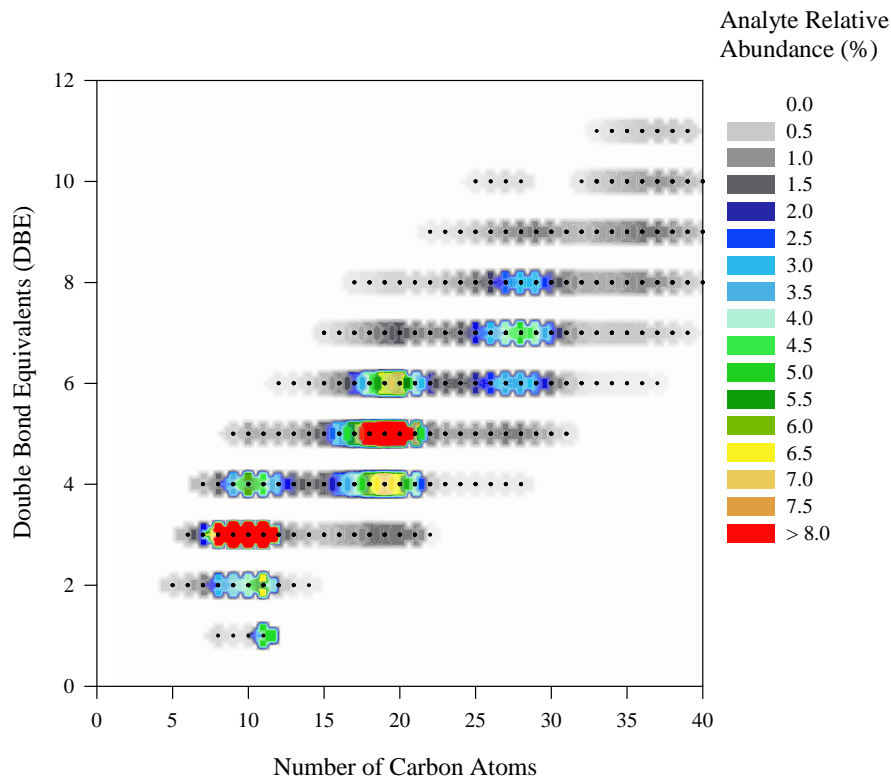


Fig. 4. Double bond equivalents (DBE) versus number of carbon atoms. The color represents the relative abundance of negative ions. Data points common between the samples with all relative abundances are included in the plots.

Characterization of limonene ozonolysis SOA

S. Kundu et al.

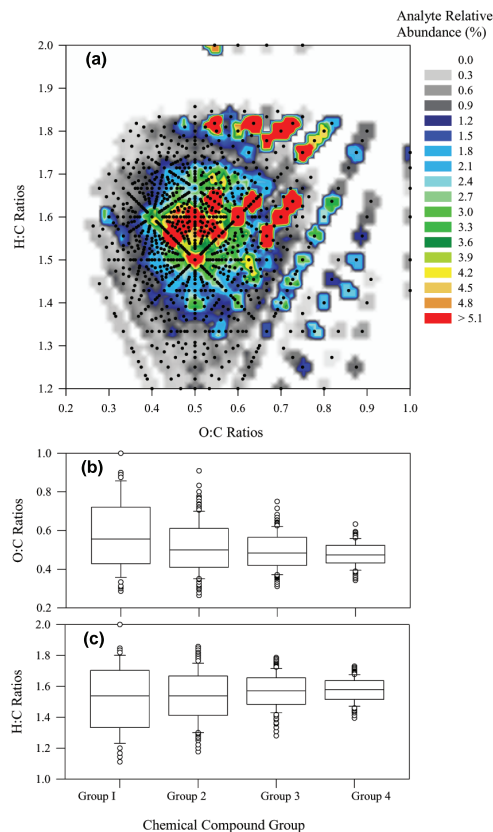


Fig. 5. (a) Depiction of the degree of oxidation for the common negative ions of the samples. Data points have been color coded according to the logarithm of their relative abundances in the mass spectrum. Boxplots (b, c) of O:C and H:C ratios are plotted with respect to the defined groups (Group I is $140 < m/z < 300$, Group II is $300 < m/z < 500$, Group III is $500 < m/z < 700$ and Group IV is $700 < m/z < 850$).

[Title Page](#)[Abstract](#)[Introduction](#)[Conclusions](#)[References](#)[Tables](#)[Figures](#)[◀](#)[▶](#)[◀](#)[▶](#)[Back](#)[Close](#)[Full Screen / Esc](#)[Printer-friendly Version](#)[Interactive Discussion](#)

Characterization of limonene ozonolysis SOA

S. Kundu et al.

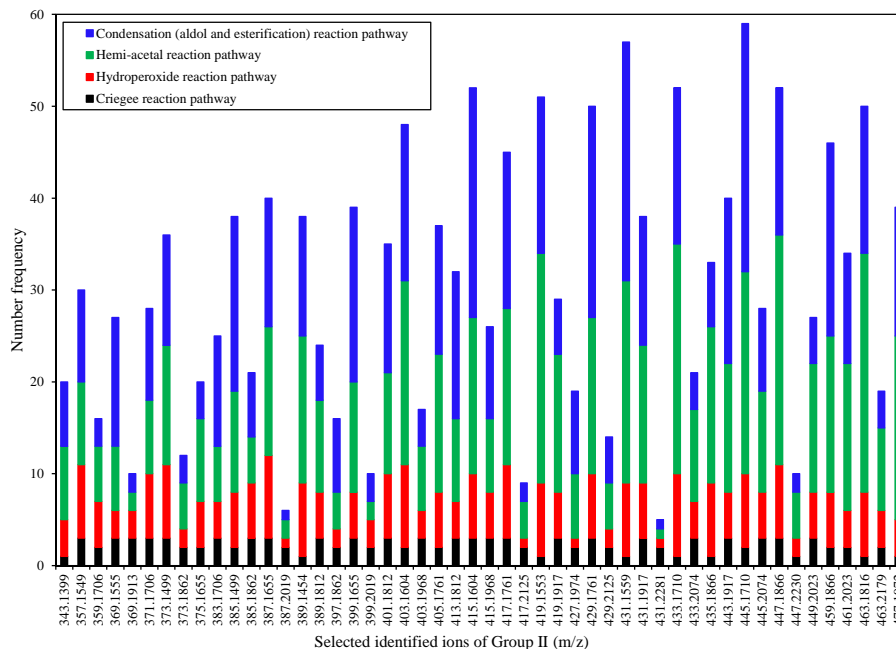


Fig. 6. Formation of the 50 most prominent Group II high MW compounds. The number frequency denotes possible combinations of building units by different reaction channels.

Title Page

Abstract

Introduction

Conclusions

References

Tables

Figures

◀

▶

◀

▶

Back

Close

Full Screen / Esc

Printer-friendly Version

Interactive Discussion



Characterization of limonene ozonolysis SOA

S. Kundu et al.

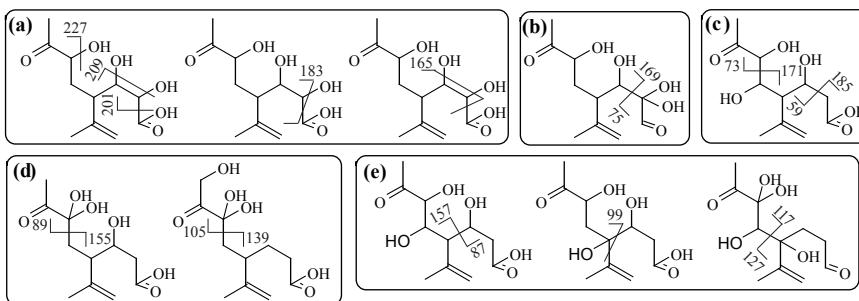
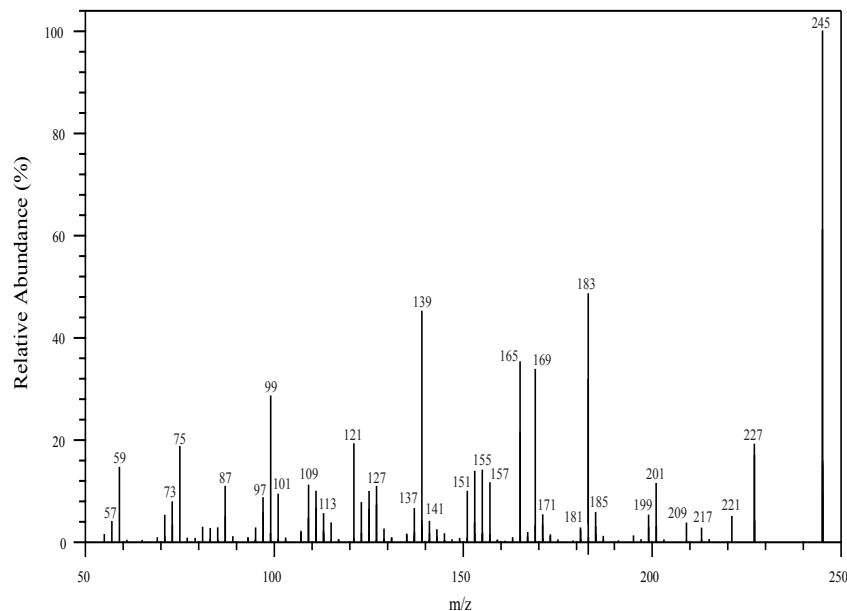


Fig. 7. Product ion mass spectrum of the fragmentation of m/z 245 ± 2 . Infrared multiphoton dissociation technique (IRMPD) was used for the fragmentation of peaks using FT ICR-MS. Proposed structural isomers and their fragmentation processes are shown in the lower panel.

Title Page

Abstract

Introduction

Conclusions

References

Tables

Figures

◀

▶

◀

▶

Back

Close

Full Screen / Esc

Printer-friendly Version

Interactive Discussion



Characterization of limonene ozonolysis SOA

S. Kundu et al.

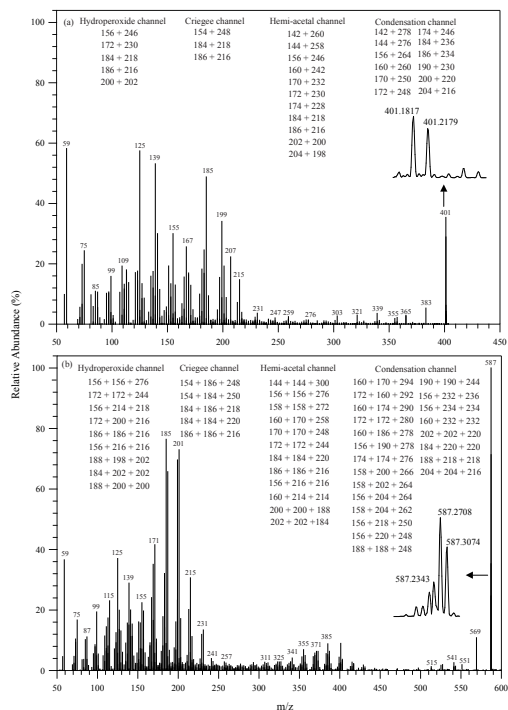


Fig. 8. (a) Product ion mass spectrum of the fragmentation of $m/z 401 \pm 2$. Infrared multiphoton dissociation technique (IRMPD) was used for the fragmentation of peaks using FT ICR-MS. The inset shows the possible combinations of building units in each of the reaction channels that could form $m/z 401.1817$ and 401.2179 . These peaks are the most prominent among the isobaric peaks at $m/z 401$. (b) Product ion mass spectrum of the fragmentation of $m/z 587 \pm 2$. Infrared multiphoton dissociation technique (IRMPD) was used for the fragmentation of peaks using FT ICR-MS. The inset shows the possible combinations of building units in each of the reaction channels that could form $m/z 587.2343$, 587.2708 and 587.3074 . These peaks are the most prominent among the isobaric peaks at $m/z 587$.